Acta Cryst E CRYSTALLOGRAPHIC COMMUNICATIONS

ISSN 2056-9890

A 2:1 co-crystal of *p*-nitrobenzoic acid and *N*,*N*′-bis(pyridin-3-ylmethyl)ethanediamide: crystal structure and Hirshfeld surface analysis

Sabrina Syed,[a] Siti Nadiah Abdul Halim,[a] Mukesh M. Jotani[b]‡ and Edward R. T. Tiekink[c]*

[a]Department of Chemistry, University of Malaya, 50603 Kuala Lumpur, Malaysia, [b]Department of Physics, Bhavan's Sheth R. A. College of Science, Ahmedabad, Gujarat 380001, India, and [c]Centre for Crystalline Materials, Faculty of Science and Technology, Sunway University, 47500 Bandar Sunway, Selangor Darul Ehsan, Malaysia. *Correspondence e-mail: edwardt@sunway.edu.my

Received 10 December 2015
Accepted 14 December 2015

Edited by W. T. A. Harrison, University of Aberdeen, Scotland

† Additional correspondence author, e-mail: mmjotani@rediffmail.com.

Keywords: crystal structure; co-crystal; hydrogen bonding; carboxylic acid; thioamide; Hirshfeld surface analysis

Supporting information: this article has supporting information at journals.iucr.org/e

The title 2:1 co-crystal, $2C_7H_5NO_4\cdot C_{14}H_{14}N_4O_2$, in which the complete diamide molecule is generated by crystallographic inversion symmetry, features a three-molecule aggregate sustained by hydroxyl-O—H···N(pyridyl) hydrogen bonds. The *p*-nitrobenzoic acid molecule is non-planar, exhibiting twists of both the carboxylic acid and nitro groups, which form dihedral angles of 10.16 (9) and 4.24 (4)°, respectively, with the benzene ring. The diamide molecule has a conformation approximating to a Z shape, with the pyridyl rings lying to either side of the central, almost planar diamide residue (r.m.s. deviation of the eight atoms being 0.025 Å), and forming dihedral angles of 77.22 (6)° with it. In the crystal, three-molecule aggregates are linked into a linear supramolecular ladder sustained by amide-N—H···O(nitro) hydrogen bonds and orientated along [10$\bar{4}$]. The ladders are connected into a double layer *via* pyridyl- and benzene-C—H···O(amide) interactions, which, in turn, are connected into a three-dimensional architecture *via* π–π stacking interactions between pyridyl and benzene rings [inter-centroid distance = 3.6947 (8) Å]. An evaluation of the Hirshfeld surfaces confirm the importance of intermolecular interactions involving oxygen atoms as well as the π–π interactions.

1. Chemical context

Arguably, the most prominent motivation for the study of co-crystals relates to their potential applications in the pharmaceutical industry whereby co-crystals of active pharmaceutical ingredients (APIs) formed with generally regarded as safe (GRAS) co-crystal coformers might provide drugs with enhanced useful properties, *e.g.* stability, solubility, bioavailability, *etc.* (Aakeröy, 2015; Almarsson & Zaworotko, 2004). Further impetus for investigating co-crystals relates to ascertaining reliable supramolecular synthons that might be exploited to direct crystal growth, or at least aggregates within crystals (Mukherjee, 2015; Tiekink, 2014). Co-crystals of *N*,*N*′-bis(pyridin-3-ylmethyl)ethanediamide, see Scheme, figured prominently in early investigations of halogen bonding (*e.g.* Goroff *et al.*, 2005) and also has been co-crystallized with carboxylic acids (*e.g.* Nguyen *et al.*, 2001). As a continuation of recent work related to the study of co-crystal formation of pyridyl-containing molecules with carboxylic acids (Arman *et al.*, 2013), the co-crystallization of *N*,*N*′-bis(pyridin-3-ylmethyl)ethanediamide with *p*-nitrobenzoic acid was investigated, yielding the title 2:1 co-crystal. The results of this investigation are reported herein.

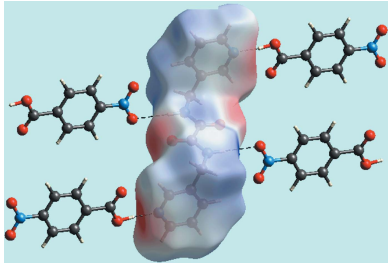

Table 1
Dihedral angles (°) for *p*-nitrobenzoic acid in the title co-crystal and in poylmorphic forms reported in the literature.

Structure	C_6/CO_2	C_6/NO_2	CO_2/NO_2	CSD refcode[a]	Ref.
*A*2/*a* form	2.37 (3)	14.82 (3)	17.34 (4)	NBZOAC04	Tonogaki *et al.* (1993)
$P2_1/m$ form	0.80 (10)	12.89 (9)	11.47 (12)	NBZOAC11	Bolte (2009)
Co-crystal	10.16 (9)	4.24 (4)	13.50 (8)	–	This work

Notes: (*a*) Groom & Allen (2014).

2. Structural commentary

The title co-crystal, Fig. 1, comprises a *p*-nitrobenzoic acid molecule (hereafter, 'acid') in a general position, and a *N*,*N*′-bis(pyridin-3-ylmethyl)ethanediamide molecule (hereafter, 'diamide') situated about a centre of inversion. This results in the 2:1 co-crystal stoichiometry.

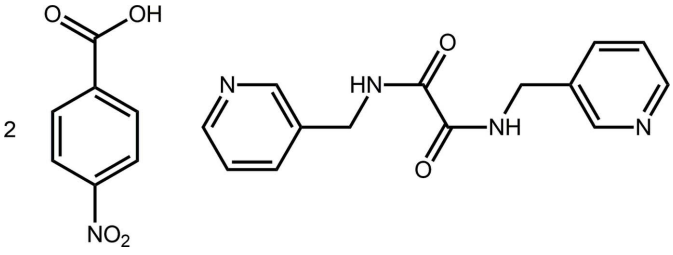

Twists are noted in the acid molecule so that the dihedral angle between the benzene ring and the non-hydrogen atoms of the carboxylic acid group is 10.16 (9)°. The comparable angle involving the nitro group is 4.24 (4)°, consistent with a smaller twist. The substituents have a conrotatory disposition forming a dihedral angle of 13.50 (8)°. The crystal structure of the free acid was first reported almost fifty years ago (Sakore & Pant, 1966) and has been the subject of several subsequent investigations. The overall conformation for the acid in the title co-crystal matches the literature structures to a first approximation but it exhibits greater and smaller twists for the carboxylic acid and nitro groups, respectively, compared to those found in the two polymorphic forms of the free acid (*A*2/*a*: Tonogaki *et al.*, 1993; $P2_1/m$: Bolte, 2009), Table 1.

The diamide features an essentially flat central residue with the r.m.s. deviation for the eight non-hydrogen atoms (O1, N2, C6 and C7, and symmetry equivalents) being 0.025 Å. This planar arrangement allows for the formation of intramolecular amide-N—H···O(amide) hydrogen bonds (Table 2). The pyridyl rings lie to either side of this plane and occupy positions approximately perpendicular to the plane, forming dihedral angles of 77.22 (6)°. Overall, the molecule has the shape of a distorted letter Z. A number of co-crystals of the diamide have been described and salient geometric parameters for these are collated in Table 3. All but one of these structures features a centrosymmetric diamide molecule. The range of dihedral angles between the central chromophore and the pendant pyridyl rings span the range 61.24 (5) to 84.6 (2)°. This conformational flexibility is reflected in the sole example of an organic salt of the diamide where the two dihedral angles vary by approximately 18°, Table 3. The other feature of these structures worth highlighting are the relatively long central C—C bond lengths, their length often resulting in a *PLATON* (Spek, 2009) alert. In the structures included in Table 3, the central C—C bond lengths vary from 1.515 (3) to 1.550 (17) Å, *cf.* 1.530 (3) Å in the title co-crystal.

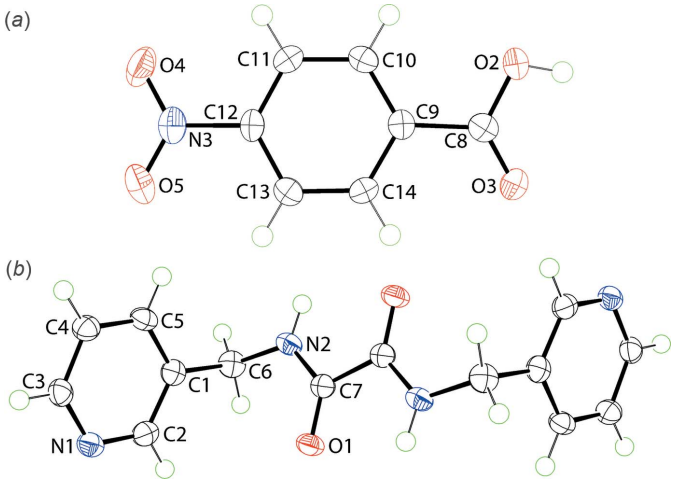

Figure 1
The molecular structures comprising the 2:1 co-crystal in the title compound showing the atom-labelling scheme and displacement ellipsoids at the 70% probability level: (*a*) *p*-nitrobenzoic acid and (*b*) *N*,*N*′-bis(pyridin-3-ylmethyl)ethanediamide; unlabelled atoms are related by the symmetry operation $2-x, 1-y, 2-z$.

3. Supramolecular features

In the packing, the anticipated (Shattock *et al.*, 2008) seven-membered {···HOCO···HCN} heterosynthon, featuring a strong hydroxy-O—H···N(pyridyl) hydrogen bond and a complementary pyridyl-C—H···O(carbonyl) interaction, is

Table 2
Hydrogen-bond geometry (Å, °).

D—H···*A*	*D*—H	H···*A*	*D*···*A*	*D*—H···*A*
N2—H2*N*···O1^{i}	0.88	2.35	2.7116 (16)	104
O2—H2*O*···N1	0.87 (1)	1.75 (1)	2.6114 (17)	175 (2)
N2—H2*N*···O5^{ii}	0.88	2.36	3.2010 (17)	159
C2—H2···O3	0.95	2.56	3.2062 (19)	125
C4—H4···O1^{iii}	0.95	2.37	3.0016 (18)	124
C5—H5···O1^{iii}	0.95	2.54	3.0843 (18)	117
C11—H11···O1^{iv}	0.95	2.45	3.2278 (18)	139

Symmetry codes: (i) $-x+2, -y+1, -z+2$; (ii) $x-1, y, z+1$; (iii) $x-1, y, z$; (iv) $-x+2, -y+1, -z+1$.

Table 3
Selected geometric details (Å, °) for *N,N′*-bis(pyridin-3-ylmethyl)ethanediamide molecules, and halogen/hydrogen bonding in its organic co-crystals and a salt.

Coformer	$C_4N_2O_2$/pyridyl	C(═O)—C(═O)	Halogen/hydrogen bonding	Refcode[a]	Ref.
p-$C_6F_4I_2$	70.56 (7)	1.544 (4)	I···O; amide-N—H···N(pyridyl)	IPOSIP	Hursthouse *et al.* (2003)
IC≡CC≡CI	76.7 (2)	1.524 (10)	I···N; amide-N—H···O(amide)	WANNOP	Goroff *et al.* (2005)
IC≡CC≡CC≡CI	84.6 (2)	1.548 (11)	I···N; amide-N—H···O(amide)	WANPIL	Goroff *et al.* (2005)
{CC(I)═C(I)C≡CC(I)═C(I)C}$_n$	80.6 (4)	1.550 (17)	I···N; amide-N—H···O(amide)	REWVUM	Jin *et al.* (2013)
$[HO_2CCH_2N(H)C(=O)]_2$	64.4 (3)	1.532 (19)	hydroxy-O—H···N(pyridyl); amide-N—H···O(amide)	CAJQAG	Nguyen *et al.* (2001)
$[HO_2CCH_2N(H)]_2C(=O)$	81.47 (6)	1.515 (3)	hydroxy-O—H···N(pyridyl); amide-N—H···O(amide)	CAJQEK	Nguyen *et al.* (2001)
$[2\text{-}(CO_2H)C_6H_4S]_2$	61.24 (5), 69.42 (6)[b]	1.534 (3)	hydroxy-O—H···N(pyridyl); amide-N—H···O(amide)	KUZSOO	Arman *et al.* (2010)
$2\text{-}NH_2C_6H_4CO_2H$	74.95 (4)	1.543 (2)	hydroxy-O—H···N(pyridyl); amide-N—H···O(carbonyl)	DIDZAT	Arman *et al.* (2012)
$2,6\text{-}(NO_2)_2C_6H_3CO_2^-$	65.31 (4), 83.22 (5)[c]	1.541 (2)	pyridinium-N—H···O(carboxylate); amide-N—H···O(carboxylate)	TIPHAD	Arman *et al.* (2013)
$4\text{-}NO_2C_6H_4CO_2H$	77.22 (6)	1.530 (3)	hydroxy-O—H···N(pyridyl)	–	This work

Notes: (*a*) Groom & Allen (2014). (*b*) The diamide molecule lacks a centre of inversion. (*c*) Salt: both pyridyl-N atoms are protonated in the non-symmetric dication.

observed, Table 2. By symmetry, each diamide molecule forms two such interactions, resulting in a centrosymmetric three molecule aggregate. To a first approximation, the components of the aggregate are co-planar with the acid molecules perpendicular to the diamide molecules, Fig. 2. This arrangement allows for the close approach of the nitro groups to the amide residues of translationally-related molecules resulting in amide-N—H···O(nitro) hydrogen bonds, and the formation of supramolecular ladders propagating along [10$\bar{4}$]. This

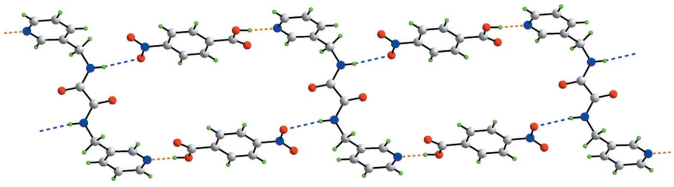

Figure 2
A view of the linear supramolecular ladder in the molecular packing of the title compound. The hydroxyl-O—H···N(pyridyl) and amide-N—H···O(nitro) hydrogen bonds are shown as orange and blue dashed lines, respectively.

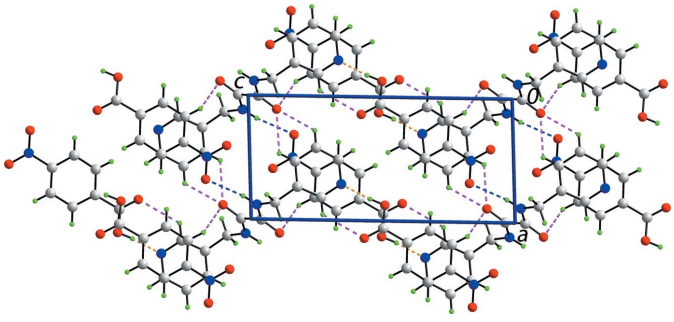

Figure 3
A view of the double layer in the title compound where the supramolecular chains shown in Fig. 2 are connected by pyridyl- and benzene-C—H···O(amide) interactions, shown as pink dashed lines. The π–π interactions within the layers (see text) are not shown.

further results in the formation of centrosymmetric 36-membered {···HOC_5NO···HNC_2NC_3N}$_2$ supramolecular rings, Fig. 2. The chains are linked into layers parallel to (010) by pyridyl-C—H···O(amide) interactions, and layers are connected into double layers by benzene-C—H···O(amide) interactions, as shown in Fig. 3. In this scheme, the amide-O1 atom accepts three close intermolecular interactions. Further consolidation within the double layers is afforded by interactions of the type π–π, which occur between centrosymmetrically related pyridyl and benzene rings, *i.e.* *Cg*(pyridyl)···*Cg*(benzene)^{i} = 3.7214 (8) Å, with an angle of 4.69 (7)° between the rings; symmetry operation: (i) 2 − *x*, 1 − *y*, 1 − *z*. The connections between the layers to consolidate the three-dimensional architecture, Fig. 4, are also of the type π–π, and also occur between centrosymmetrically related pyridyl and benzene rings, *i.e.* *Cg*(pyridyl)···*Cg*(benzene)^{ii} = 3.6947 (8) Å with an angle of inclination = 4.69 (7)°; symmetry operation: (ii) 2 − *x*, 2 − *y*, 1 − *z*.

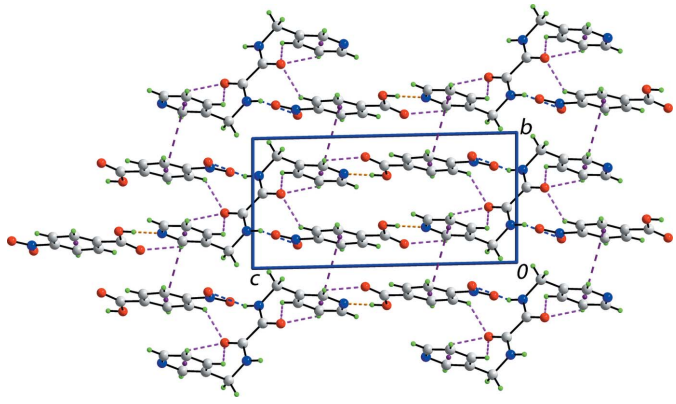

Figure 4
A view of the unit-cell contents of the title compound shown in projection down the *a* axis, whereby the supramolecular layers, illustrated in Fig. 3, are linked by π–π interactions, shown as purple dashed lines, leading to a three-dimensional architecture.

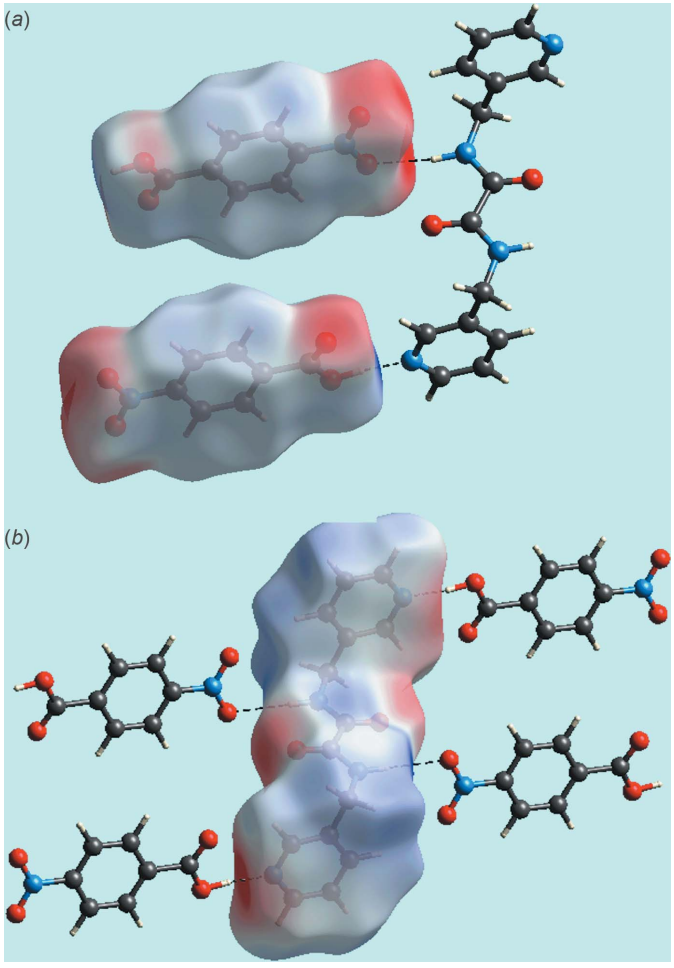

Figure 5
Views of the Hirshfeld surfaces mapped over the calculated electrostatic potential: (*a*) acid and (*b*) diamide in the title compound.

4. Analysis of the Hirshfeld surfaces

The packing of the title compound was also investigated by an analysis of the Hirshfeld surfaces (Spackman & Jayatilaka, 2009) with the aid of *CrystalExplorer* (Wolff *et al.*, 2012). The two-dimensional fingerprint plots (Rohl *et al.*, 2008) were calculated for the crystal as well as for the individual coformers, as were the electrostatic potentials using *TONTO* (Spackman *et al.*, 2008; Jayatilaka *et al.*, 2005), also with *CrystalExplorer*; the electrostatic potentials were mapped on the Hirshfeld surfaces using the STO–3G basis set at the level of Hartree–Fock theory over a range of ±0.075 au.

The presence of strong hydroxyl-O—H···N(pyridyl) and amide-N—H···O(nitro) interactions between the pair of acid molecules and a diamide molecule can be observed through their corresponding Hirshfeld surfaces mapped over the electrostatic potential, Fig. 5. From symmetry, each diamide forms two pairs of interactions, visualized as bright-red spots on the Hirshfeld surface mapped over $d_{\rm norm}$ and labelled as 1 and 3, respectively, in Fig. 6. The full fingerprint plot for the co-crystal is shown in Fig. 7. The prominent spikes at $d_e + d_i$ = 1.6 Å are due to N···H/H···N contacts. Thus, the long spike in the upper left region is due to the hydroxyl-O—H···N(pyridyl) interaction and the similar long spike at the same $d_e + d_i$ distance in the lower right region indicates the contribution of the amide-N—H···O(nitro) interaction. The donor–acceptor contributions of these co-crystal constituents are highlighted with the label 'd′ in the fingerprint plot, Fig. 7. The intermolecular O···H and H···O contacts, which are prominent in the molecular packing, Table 2 and Fig. 5, provide quite different contributions to the Hirshfeld surfaces of the acid and diamide molecules. While the O···H contacts have a large contribution, *i.e.* 32.3%, to the Hirshfeld surface of the acid, a smaller contribution, *i.e.* 8.3%, is provided by the diamide; the reverse is true for for the O···H contacts, *i.e.* 8.5 and 30.4%, respectively. The overall fingerprint plot for the co-crystal when delineated into O···H/H···O contacts leads to the pair of spikes corresponding to donors and acceptors

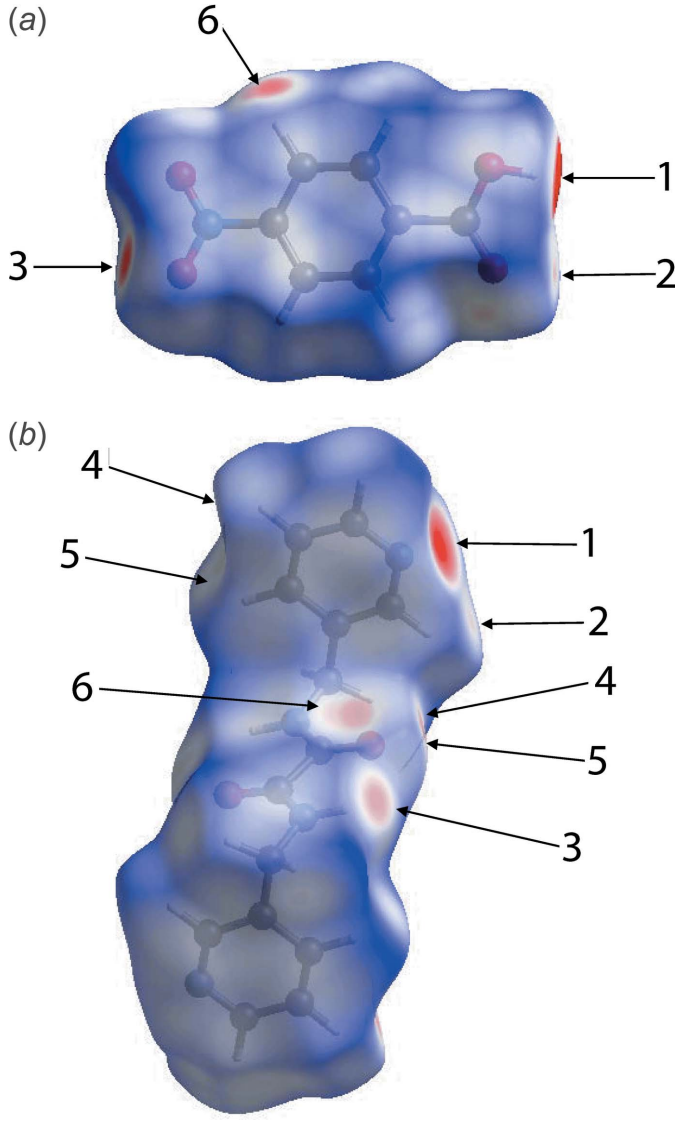

Figure 6
Views of the Hirshfeld surface mapped over $d_{\rm norm}$: (*a*) acid and (*b*) diamide in the title compound.

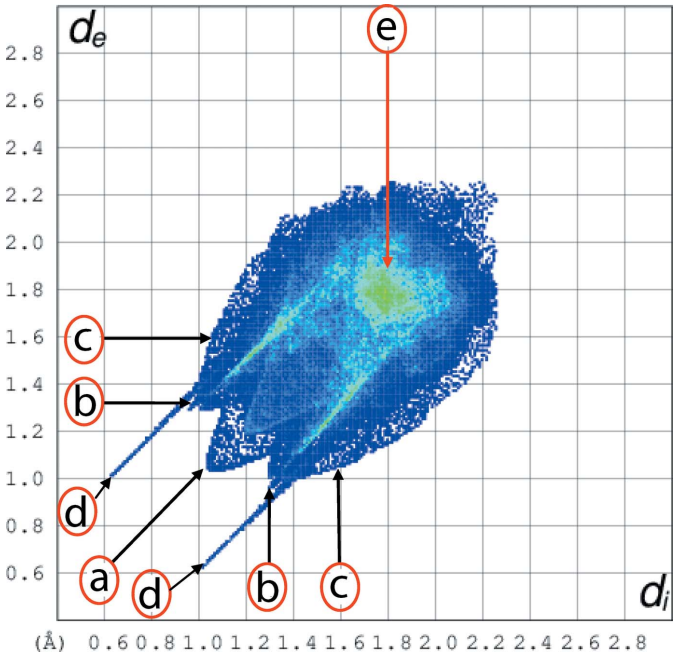

Figure 7
The two-dimensional fingerprint plot for the title 2:1 co-crystal showing contributions from different contacts: (a) H···H, (b) O···H/H···O, (c) C···H/H···C, (d) N···H/H···N and (e) C···C.

with a 37.1% contribution to surface (featured as 'b' in Fig. 7). The donors and acceptors corresponding to intermolecular C—H···O interactions are seen as pale-red spots and are labelled as 2, 4, 5 and 6 in Fig. 6. The contribution from C···H/H···C contacts (10.4% of the Hirshfeld surface) results in a symmetrical pair of wings, see 'c' in Fig. 7. The C···C contacts assigned to π–π stacking interactions appear as a distinct triangle in the fingerprint plot, see 'e' in Fig. 7, at around $d_e = d_i = 1.8$ Å. The presence of these π–π stacking interactions is justified by the appearance of red and blue triangle pairs on the Hirshfeld surface mapped with shape index identified with arrows in the images of Fig. 8 and in the flat regions on the Hirshfeld surfaces mapped with curvedness in Fig. 9. The H···H contacts appear as the scattered points along with a single broad peak in the middle region of the fingerprint plot for each of the co-crystal constituents; the peak positions are at $d_e = d_i = 1.2$ and 1.0 Å, and the % contributions are 24.3% and 29.7% for acid and diamide, respectively. Thus, the overall 28.6% contribution to the Hirshfeld surface of the co-crystal is just the superimposition of these individual fingerprint plots, and results in the peak marked with 'a' in Fig. 7. The relative contributions from

Table 4
Percentage contribution of the different intermolecular interactions to the Hirshfeld surfaces for the acid, diamide and co-crystal.

Interaction	Acid	Diamide	Co-crystal
H···H	24.3	29.7	28.6
O···H/H···O	40.8	38.7	37.1
C···H/H···C	10.5	7.6	10.4
N···H/H···N	4.5	8.2	4.4
C···C	6.5	7.0	7.2
C···N/N···C	4.4	4.6	5.0
C···O/O···C	6.5	3.1	5.4
N···O/O···N	0.4	0.4	0.4
O···O	2.1	0.7	1.5

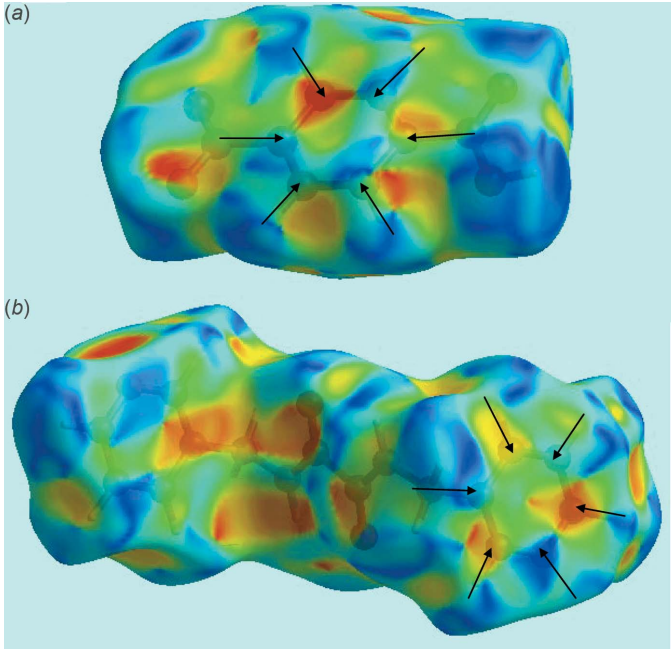

Figure 8
Hirshfeld surfaces mapped over the shape index for (*a*) the acid and (*b*) the diamide, highlighting the regions involved in π–π stacking interactions.

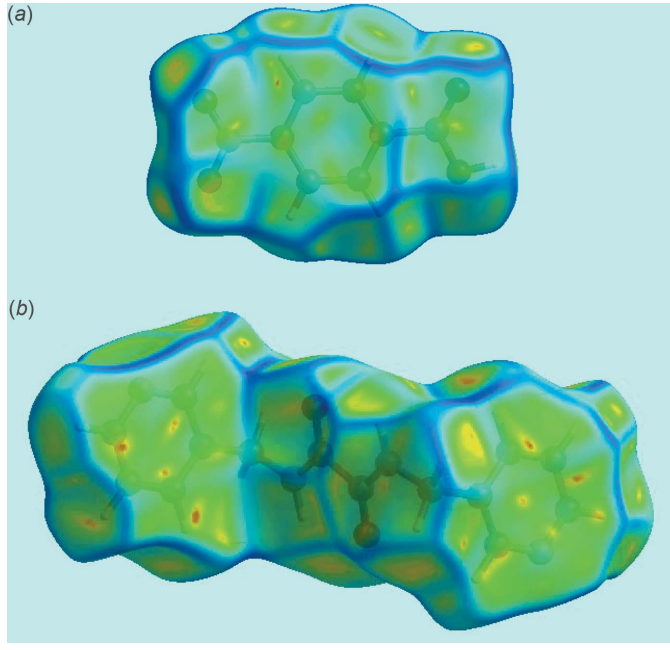

Figure 9
Hirshfeld surfaces mapped over curvedness for (*a*) the acid and (*b*) the diamide, highlighting the regions involved in π–π stacking interactions.

Table 5
Enrichment ratios (ER) for the acid, diamide and co-crystal.

Interaction	Acid	Diamide	Co-crystal
H···H	0.89	0.92	0.96
O···H·H···O	1.55	1.56	1.48
C···H/H···C	0.59	0.46	0.54
N···H/H···N	0.94	1.09	0.82
C···C	3.26	2.20	2.90

various contacts to the Hirshfeld surfaces of acid, diamide and the co-crystal are tabulated in Table 4.

A further analysis of Hirshfeld surfaces was conducted using a new descriptor, *i.e.* the enrichment ratio, ER (Jelsch *et al.*, 2014), Table 5. The ER relates to the propensity of chemical species to form specific interactions in the molecular packing. The ER value of approximately 1.5 for the O···H/H···O contacts clearly provides evidence for the formation of O—H···N, N—H···O and C—H···O interactions. The high propensity of *N*-heterocycles, *e.g.* pyridyl, to form π–π stacking interactions with benzene is also evident from the high ER values corresponding to C···C contacts in the structure. On the other hand, the values of ER, *i.e.* < 0.6, reflects the low propensity for C···H/H···C contacts in the structure as the result of significant interactions involving O···H and N···H contacts. The enrichment ratios are closer to unity for the N···H/H···N contacts, an observation that is consistent with their relatively low contribution to the overall surface area. Finally, ER values close to but slightly less than unity for the H···H contacts are noted, in accord with expectation (Jelsch *et al.*, 2014). The ER values for other contacts are of low significance as they are derived from less important interactions with small contributions to the overall Hirshfeld surface.

5. Database survey

As mentioned in the *Chemical context*, the diamide investigated herein has been the subject of several co-crystallization investigations, *i.e.* with co-formers capable of forming both halogen bonding and conventional hydrogen bonding interactions. Referring to the data in Table 3, three of the co-crystals having an iodide substituent in the co-former, feature N···I halogen bonding along with amide-N—H···O(amide) hydrogen bonding, the latter leading to amide 'tapes'. The exceptional structure is found in the 1:1 co-crystal with *p*-$C_6F_4I_2$ where I···O halogen bonding and amide-N—H···N(pyridyl) hydrogen bonding was observed (Hursthouse *et al.*, 2003). In co-crystals with carboxylic acids, hydroxy-O—H···N(pyridyl) hydrogen bonding complementing amide-N—H···N(pyridyl) mediated tapes is normally observed. In the exceptional structure, *i.e.* of the 2:1 co-crystal with anthranilic acid, amide-N—H···O(carbonyl) hydrogen bonding is seen along with hydroxy-O—H···N(pyridyl) hydrogen bonding (Arman *et al.*, 2012). Finally, one salt has been reported with the 2,6-$(NO_2)_2C_6H_3CO_2^-$ anion (Arman *et al.*, 2013). Here, charge-assisted pyridinium-N—H···O(carboxylate) and amide-N—H···O(carboxylate) hydrogen bonding is found.

Table 6
Experimental details.

Crystal data	
Chemical formula	$C_{14}H_{14}N_4O_2{\cdot}2C_7H_5NO_4$
M_r	604.53
Crystal system, space group	Triclinic, $P\overline{1}$
Temperature (K)	100
a, b, c (Å)	6.6981 (4), 6.9988 (4), 14.1770 (9)
α, β, γ (°)	91.070 (5), 92.131 (5), 96.602 (5)
V (Å^3)	659.56 (7)
Z	1
Radiation type	Mo $K\alpha$
μ (mm^{-1})	0.12
Crystal size (mm)	0.30 × 0.25 × 0.20
Data collection	
Diffractometer	Agilent SuperNova Dual diffractometer with Atlas detector
Absorption correction	Multi-scan (*CrysAlis PRO*; Agilent, 2014)
T_{min}, T_{max}	0.633, 1.000
No. of measured, independent and observed [$I > 2\sigma(I)$] reflections	5870, 2645, 2203
R_{int}	0.021
(sin $\theta/\lambda)_{max}$ (Å^{-1})	0.628
Refinement	
$R[F^2 > 2\sigma(F^2)]$, $wR(F^2)$, S	0.040, 0.110, 1.05
No. of reflections	2645
No. of parameters	202
No. of restraints	2
$\Delta\rho_{max}$, $\Delta\rho_{min}$ (e Å^{-3})	0.37, −0.25

Computer programs: *CrysAlis PRO* (Agilent, 2014), *SHELXS97* (Sheldrick, 2008), *SHELXL2014/7* (Sheldrick, 2015), *ORTEP-3 for Windows* (Farrugia, 2012), *QMol* (Gans & Shalloway, 2001), *DIAMOND* (Brandenburg, 2006) and *publCIF* (Westrip, 2010).

6. Synthesis and crystallization

The diamide (0.5 mmol), prepared in accord with the literature procedure (Schauer *et al.*, 1997), in ethanol (5 ml) was added to a ethanol solution (5 ml) of 4-nitrobenzoic acid (Merck, 0.5 mmol). The mixture was stirred for 3 h at room temperature. After standing for a few minutes, a white precipitate formed which was filtered off by vacuum suction. The filtrate was then left at room temperature, yielding colourless blocks of the title compound after 2 weeks.

7. Refinement

Crystal data, data collection and structure refinement details are summarized in Table 6. The carbon-bound H-atoms were placed in calculated positions (C—H = 0.95–0.99 Å) and were included in the refinement in the riding model approximation, with U_{iso}(H) set to 1.2U_{equiv}(C). The oxygen- and nitrogen-bound H-atoms were located in a difference Fourier map but were refined with distance restraints of O—H = 0.84±0.01 Å and N—H = 0.88±0.01 Å, and with U_{iso}(H) set to 1.5U_{eq}(O) and 1.2U_{eq}(N).

Acknowledgements

The authors thank the Exploratory Research Grant Scheme (ER008-2013A) for support.

References

Aakeröy, C. (2015). *Acta Cryst.* B**71**, 387–391.
Agilent (2014). *CrysAlis PRO*. Agilent Technologies Inc., Santa Clara, CA, USA.
Almarsson, Ö. & Zaworotko, M. J. (2004). *Chem. Commun*. pp. 1889–1896.
Arman, H. D., Miller, T. & Tiekink, E. R. T. (2012). *Z. Kristallogr*. **227**, 825–830.
Arman, H. D., Miller, T., Poplaukhin, P. & Tiekink, E. R. T. (2010). *Acta Cryst.* E**66**, o2590–o2591.
Arman, H. D., Miller, T., Poplaukhin, P. & Tiekink, E. R. T. (2013). *Z. Kristallogr.* **228**, 295–303.
Bolte, M. (2009). Private communication to the CCDC, Cambridge, England.
Brandenburg, K. (2006). *DIAMOND*. Crystal Impact GbR, Bonn, Germany.
Farrugia, L. J. (2012). *J. Appl. Cryst.* **45**, 849–854.
Gans, J. & Shalloway, D. (2001). *J. Mol. Graphics Modell.* **19**, 557–559.
Goroff, N. S., Curtis, S. M., Webb, J. A., Fowler, F. W. & Lauher, J. W. (2005). *Org. Lett.* **7**, 1891–1893.
Groom, C. R. & Allen, F. H. (2014). *Angew. Chem. Int. Ed.* **53**, 662–671.
Hursthouse, M. B., Gelbrich, T. & Plater, M. J. (2003). Private Communication to the CSD .
Jayatilaka, D., Grimwood, D. J., Lee, A., Lemay, A., Russel, A. J., Taylor, C., Wolff, S. K., Cassam-Chenai, P. & Whitton, A. (2005). *TONTO – A System for Computational Chemistry*. Available at: http://hirshfeldsurface.net/
Jelsch, C., Ejsmont, K. & Huder, L. (2014). *IUCrJ*, **1**, 119–128.
Jin, H., Plonka, A. M., Parise, J. B. & Goroff, N. S. (2013). *CrystEngComm*, **15**, 3106–3110.
Mukherjee, A. (2015). *Cryst. Growth Des.* **15**, 3076–3085.
Nguyen, T. L., Fowler, F. W. & Lauher, J. W. (2001). *J. Am. Chem. Soc.* **123**, 11057–11064.
Rohl, A. L., Moret, M., Kaminsky, W., Claborn, K., McKinnon, J. J. & Kahr, B. (2008). *Cryst. Growth Des.* **8**, 4517–4525.
Sakore, T. D. & Pant, L. M. (1966). *Acta Cryst.* **21**, 715–719.
Schauer, C. L., Matwey, E., Fowler, F. W. & Lauher, J. W. (1997). *J. Am. Chem. Soc.* **119**, 10245–10246.
Shattock, T., Arora, K. K., Vishweshwar, P. & Zaworotko, M. J. (2008). *Cryst. Growth Des.* **8**, 4533–4545.
Sheldrick, G. M. (2008). *Acta Cryst.* A**64**, 112–122.
Sheldrick, G. M. (2015). *Acta Cryst.* C**71**, 3–8.
Spackman, M. A. & Jayatilaka, D. (2009). *CrystEngComm*, **11**, 19–32.
Spackman, M. A., McKinnon, J. J. & Jayatilaka, D. (2008). *CrystEngComm*, **10**, 377–388.
Spek, A. L. (2009). *Acta Cryst.* D**65**, 148–155.
Tiekink, E. R. T. (2014). *Chem. Commun.* **50**, 11079–11082.
Tonogaki, M., Kawata, T., Ohba, S., Iwata, Y. & Shibuya, I. (1993). *Acta Cryst.* B**49**, 1031–1039.
Westrip, S. P. (2010). *J. Appl. Cryst.* **43**, 920–925.
Wolff, S. K., Grimwood, D. J., McKinnon, J. J., Turner, M. J., Jayatilaka, D. & Spackman, M. A. (2012). *Crystal Explorer*. The University of Western Australia.

supporting information

Acta Cryst. (2016). E**72**, 76-82 [doi:10.1107/S2056989015024068]

A 2:1 co-crystal of *p*-nitrobenzoic acid and *N*,*N*′-bis(pyridin-3-ylmethyl)-ethanediamide: crystal structure and Hirshfeld surface analysis

Sabrina Syed, Siti Nadiah Abdul Halim, Mukesh M. Jotani and Edward R. T. Tiekink

Computing details

Data collection: *CrysAlis PRO* (Agilent, 2014); cell refinement: *CrysAlis PRO* (Agilent, 2014); data reduction: *CrysAlis PRO* (Agilent, 2014); program(s) used to solve structure: *SHELXS97* (Sheldrick, 2008); program(s) used to refine structure: *SHELXL2014*/7 (Sheldrick, 2015); molecular graphics: *ORTEP-3 for Windows* (Farrugia, 2012), *QMol* (Gans & Shalloway, 2001), *DIAMOND* (Brandenburg, 2006); software used to prepare material for publication: *publCIF* (Westrip, 2010).

4-Nitrobenzoic acid–*N*,*N*′-bis(pyridin-3-ylmethyl)ethanediamide (2/1)

Crystal data

$C_{14}H_{14}N_4O_2·2C_7H_5NO_4$
M_r = 604.53
Triclinic, $P\overline{1}$
a = 6.6981 (4) Å
b = 6.9988 (4) Å
c = 14.1770 (9) Å
α = 91.070 (5)°
β = 92.131 (5)°
γ = 96.602 (5)°
V = 659.56 (7) Å^3
Z = 1
$F(000)$ = 314
D_x = 1.522 Mg m^{-3}
Mo $K\alpha$ radiation, λ = 0.71073 Å
Cell parameters from 2741 reflections
θ = 4.0–28.8°
μ = 0.12 mm^{-1}
T = 100 K
Block, colourless
0.30 × 0.25 × 0.20 mm

Data collection

Agilent SuperNova Dual diffractometer with Atlas detector
Radiation source: SuperNova (Mo) X-ray Source
Mirror monochromator
Detector resolution: 10.4041 pixels mm^{-1}
ω scan
Absorption correction: multi-scan (*CrysAlis PRO*; Agilent, 2014)
T_{min} = 0.633, T_{max} = 1.000
5870 measured reflections
2645 independent reflections
2203 reflections with $I > 2\sigma(I)$
R_{int} = 0.021
θ_{max} = 26.5°, θ_{min} = 2.9°
h = −8→8
k = −8→8
l = −17→16

Refinement

Refinement on F^2
Least-squares matrix: full
$R[F^2 > 2\sigma(F^2)]$ = 0.040
$wR(F^2)$ = 0.110
S = 1.05
2645 reflections
202 parameters
2 restraints
Hydrogen site location: mixed
$w = 1/[\sigma^2(F_o^2) + (0.0513P)^2 + 0.2196P]$ where $P = (F_o^2 + 2F_c^2)/3$
$(\Delta/\sigma)_{max} < 0.001$
$\Delta\rho_{max}$ = 0.37 e Å^{-3}
$\Delta\rho_{min}$ = −0.25 e Å^{-3}

Special details

Geometry. All esds (except the esd in the dihedral angle between two l.s. planes) are estimated using the full covariance matrix. The cell esds are taken into account individually in the estimation of esds in distances, angles and torsion angles; correlations between esds in cell parameters are only used when they are defined by crystal symmetry. An approximate (isotropic) treatment of cell esds is used for estimating esds involving l.s. planes.

Fractional atomic coordinates and isotropic or equivalent isotropic displacement parameters (Å²)

	x	*y*	*z*	U_{iso}*/U_{eq}
O1	1.11011 (16)	0.56895 (15)	0.89399 (7)	0.0199 (3)
N1	0.70817 (19)	0.71283 (17)	0.65579 (9)	0.0186 (3)
N2	0.88281 (19)	0.71178 (17)	0.97708 (9)	0.0179 (3)
H2N	0.8149	0.7109	1.0291	0.021*
C1	0.7342 (2)	0.7881 (2)	0.82222 (11)	0.0172 (3)
C2	0.8169 (2)	0.7782 (2)	0.73381 (11)	0.0183 (3)
H2	0.9561	0.8193	0.7284	0.022*
C3	0.5122 (2)	0.6562 (2)	0.66314 (11)	0.0187 (3)
H3	0.4350	0.6101	0.6081	0.022*
C4	0.4177 (2)	0.6621 (2)	0.74804 (11)	0.0194 (3)
H4	0.2778	0.6218	0.7510	0.023*
C5	0.5299 (2)	0.7276 (2)	0.82860 (11)	0.0178 (3)
H5	0.4680	0.7313	0.8877	0.021*
C6	0.8627 (2)	0.8617 (2)	0.90832 (11)	0.0204 (3)
H6A	0.9980	0.9132	0.8883	0.024*
H6B	0.8018	0.9684	0.9386	0.024*
C7	1.0031 (2)	0.5762 (2)	0.96193 (10)	0.0155 (3)
O2	0.87273 (16)	0.69092 (16)	0.49240 (8)	0.0215 (3)
H2O	0.825 (3)	0.698 (3)	0.5481 (8)	0.032*
O3	1.14230 (17)	0.83861 (17)	0.57361 (8)	0.0250 (3)
O4	1.41048 (19)	0.74597 (18)	0.08648 (8)	0.0315 (3)
O5	1.68626 (18)	0.82597 (18)	0.16957 (8)	0.0298 (3)
N3	1.5028 (2)	0.78448 (18)	0.16264 (9)	0.0218 (3)
C8	1.0608 (2)	0.7690 (2)	0.50090 (11)	0.0183 (3)
C9	1.1723 (2)	0.7669 (2)	0.41044 (10)	0.0163 (3)
C10	1.0748 (2)	0.7181 (2)	0.32349 (11)	0.0181 (3)
H10	0.9339	0.6801	0.3201	0.022*
C11	1.1823 (2)	0.7246 (2)	0.24197 (11)	0.0180 (3)
H11	1.1166	0.6924	0.1823	0.022*
C12	1.3883 (2)	0.7791 (2)	0.24931 (10)	0.0166 (3)
C13	1.4902 (2)	0.8288 (2)	0.33481 (11)	0.0180 (3)
H13	1.6310	0.8672	0.3379	0.022*
C14	1.3796 (2)	0.8204 (2)	0.41546 (11)	0.0169 (3)
H14	1.4458	0.8516	0.4751	0.020*

Atomic displacement parameters (Å²)

	U^{11}	U^{22}	U^{33}	U^{12}	U^{13}	U^{23}
O1	0.0189 (6)	0.0249 (6)	0.0158 (5)	0.0010 (4)	0.0052 (5)	0.0015 (4)

N1	0.0224 (7)	0.0171 (6)	0.0176 (7)	0.0061 (5)	0.0044 (6)	0.0030 (5)
N2	0.0194 (7)	0.0203 (6)	0.0138 (6)	0.0013 (5)	0.0032 (5)	−0.0007 (5)
C1	0.0206 (8)	0.0118 (6)	0.0196 (8)	0.0035 (6)	0.0012 (6)	0.0025 (6)
C2	0.0178 (8)	0.0149 (7)	0.0229 (8)	0.0031 (6)	0.0035 (6)	0.0045 (6)
C3	0.0211 (8)	0.0183 (7)	0.0174 (8)	0.0048 (6)	0.0000 (6)	0.0028 (6)
C4	0.0182 (8)	0.0191 (7)	0.0207 (8)	0.0010 (6)	0.0029 (6)	0.0032 (6)
C5	0.0208 (8)	0.0164 (7)	0.0169 (7)	0.0027 (6)	0.0053 (6)	0.0025 (6)
C6	0.0217 (8)	0.0166 (7)	0.0225 (8)	0.0003 (6)	0.0013 (7)	0.0009 (6)
C7	0.0133 (7)	0.0181 (7)	0.0138 (7)	−0.0025 (6)	−0.0017 (6)	−0.0040 (6)
O2	0.0197 (6)	0.0264 (6)	0.0185 (6)	0.0011 (5)	0.0052 (5)	0.0008 (5)
O3	0.0243 (6)	0.0333 (6)	0.0169 (6)	0.0014 (5)	0.0027 (5)	−0.0040 (5)
O4	0.0396 (8)	0.0406 (7)	0.0152 (6)	0.0078 (6)	0.0037 (5)	−0.0007 (5)
O5	0.0234 (7)	0.0353 (7)	0.0321 (7)	0.0051 (5)	0.0115 (5)	0.0037 (5)
N3	0.0273 (8)	0.0183 (6)	0.0215 (7)	0.0070 (6)	0.0066 (6)	0.0029 (5)
C8	0.0179 (8)	0.0158 (7)	0.0214 (8)	0.0031 (6)	0.0002 (6)	0.0027 (6)
C9	0.0190 (8)	0.0126 (7)	0.0177 (8)	0.0029 (6)	0.0025 (6)	0.0017 (6)
C10	0.0153 (7)	0.0162 (7)	0.0225 (8)	0.0010 (6)	0.0003 (6)	−0.0003 (6)
C11	0.0217 (8)	0.0163 (7)	0.0158 (7)	0.0024 (6)	−0.0024 (6)	−0.0004 (6)
C12	0.0212 (8)	0.0135 (7)	0.0161 (7)	0.0044 (6)	0.0052 (6)	0.0018 (6)
C13	0.0163 (8)	0.0161 (7)	0.0216 (8)	0.0022 (6)	0.0010 (6)	0.0011 (6)
C14	0.0190 (8)	0.0155 (7)	0.0158 (7)	0.0016 (6)	−0.0024 (6)	−0.0004 (6)

Geometric parameters (Å, º)

O1—C7	1.2256 (17)	O2—C8	1.3145 (18)
N1—C3	1.335 (2)	O2—H2O	0.867 (9)
N1—C2	1.344 (2)	O3—C8	1.2150 (18)
N2—C7	1.3329 (19)	O4—N3	1.2338 (18)
N2—C6	1.4594 (19)	O5—N3	1.2294 (18)
N2—H2N	0.8800	N3—C12	1.4713 (19)
C1—C2	1.393 (2)	C8—C9	1.508 (2)
C1—C5	1.392 (2)	C9—C10	1.392 (2)
C1—C6	1.514 (2)	C9—C14	1.395 (2)
C2—H2	0.9500	C10—C11	1.383 (2)
C3—C4	1.383 (2)	C10—H10	0.9500
C3—H3	0.9500	C11—C12	1.388 (2)
C4—C5	1.384 (2)	C11—H11	0.9500
C4—H4	0.9500	C12—C13	1.387 (2)
C5—H5	0.9500	C13—C14	1.384 (2)
C6—H6A	0.9900	C13—H13	0.9500
C6—H6B	0.9900	C14—H14	0.9500
C7—C7^{i}	1.530 (3)		
C3—N1—C2	118.66 (13)	N2—C7—C7^{i}	113.82 (15)
C7—N2—C6	120.64 (13)	C8—O2—H2O	106.0 (13)
C7—N2—H2N	119.7	O5—N3—O4	123.07 (14)
C6—N2—H2N	119.7	O5—N3—C12	118.45 (13)
C2—C1—C5	117.70 (14)	O4—N3—C12	118.48 (13)

C2—C1—C6	121.03 (14)	O3—C8—O2	124.77 (14)
C5—C1—C6	121.28 (14)	O3—C8—C9	121.32 (13)
N1—C2—C1	122.83 (14)	O2—C8—C9	113.91 (13)
N1—C2—H2	118.6	C10—C9—C14	119.84 (14)
C1—C2—H2	118.6	C10—C9—C8	122.27 (13)
N1—C3—C4	122.32 (14)	C14—C9—C8	117.88 (13)
N1—C3—H3	118.8	C11—C10—C9	120.24 (14)
C4—C3—H3	118.8	C11—C10—H10	119.9
C3—C4—C5	119.07 (14)	C9—C10—H10	119.9
C3—C4—H4	120.5	C10—C11—C12	118.52 (14)
C5—C4—H4	120.5	C10—C11—H11	120.7
C4—C5—C1	119.42 (14)	C12—C11—H11	120.7
C4—C5—H5	120.3	C13—C12—C11	122.73 (14)
C1—C5—H5	120.3	C13—C12—N3	118.79 (13)
N2—C6—C1	112.31 (12)	C11—C12—N3	118.48 (13)
N2—C6—H6A	109.1	C14—C13—C12	117.71 (14)
C1—C6—H6A	109.1	C14—C13—H13	121.1
N2—C6—H6B	109.1	C12—C13—H13	121.1
C1—C6—H6B	109.1	C13—C14—C9	120.96 (14)
H6A—C6—H6B	107.9	C13—C14—H14	119.5
O1—C7—N2	124.82 (14)	C9—C14—H14	119.5
O1—C7—C7^{i}	121.36 (17)		

C3—N1—C2—C1	0.5 (2)	O2—C8—C9—C14	−170.76 (12)
C5—C1—C2—N1	−0.2 (2)	C14—C9—C10—C11	−0.8 (2)
C6—C1—C2—N1	179.66 (13)	C8—C9—C10—C11	177.77 (13)
C2—N1—C3—C4	−0.1 (2)	C9—C10—C11—C12	0.5 (2)
N1—C3—C4—C5	−0.5 (2)	C10—C11—C12—C13	−0.5 (2)
C3—C4—C5—C1	0.8 (2)	C10—C11—C12—N3	179.50 (12)
C2—C1—C5—C4	−0.4 (2)	O5—N3—C12—C13	2.7 (2)
C6—C1—C5—C4	179.72 (13)	O4—N3—C12—C13	−177.78 (13)
C7—N2—C6—C1	75.28 (17)	O5—N3—C12—C11	−177.38 (13)
C2—C1—C6—N2	−113.64 (15)	O4—N3—C12—C11	2.2 (2)
C5—C1—C6—N2	66.21 (18)	C11—C12—C13—C14	0.8 (2)
C6—N2—C7—O1	3.1 (2)	N3—C12—C13—C14	−179.25 (12)
C6—N2—C7—C7^{i}	−176.55 (14)	C12—C13—C14—C9	−1.0 (2)
O3—C8—C9—C10	−168.99 (14)	C10—C9—C14—C13	1.0 (2)
O2—C8—C9—C10	10.7 (2)	C8—C9—C14—C13	−177.57 (13)
O3—C8—C9—C14	9.6 (2)		

Symmetry code: (i) −*x*+2, −*y*+1, −*z*+2.

Hydrogen-bond geometry (Å, º)

D—H···*A*	*D*—H	H···*A*	*D*···*A*	*D*—H···*A*
N2—H2*N*···O1^{i}	0.88	2.35	2.7116 (16)	104
O2—H2*O*···N1	0.87 (1)	1.75 (1)	2.6114 (17)	175 (2)
N2—H2*N*···O5^{ii}	0.88	2.36	3.2010 (17)	159

C2—H2···O3	0.95	2.56	3.2062 (19)	125
C4—H4···O1^{iii}	0.95	2.37	3.0016 (18)	124
C5—H5···O1^{iii}	0.95	2.54	3.0843 (18)	117
C11—H11···O1^{iv}	0.95	2.45	3.2278 (18)	139

Symmetry codes: (i) −*x*+2, −*y*+1, −*z*+2; (ii) *x*−1, *y*, *z*+1; (iii) *x*−1, *y*, *z*; (iv) −*x*+2, −*y*+1, −*z*+1.